Using Instrumented Indentation to Measure the Complex Modulus of Highly Plasticized Polyvinyl Chloride

Application Note

Jennifer Hay

The Agilent G200 Nanoindenter.

Introduction

Polymers are often employed in engineering designs because of their ability to damp out shock and vibration. Rubber tires certainly provide a more comfortable ride than wooden wagon wheels! A materials' ability to elastically store energy is characterized by the storage modulus (E'); the ability to damp is characterized by the loss modulus (E''). The *complex modulus* (E^*) is often used to characterize polymers, because it incorporates both of these capacities:

$$E^* = E' + iE''.$$

For bulk samples of material, complex modulus can be measured using dynamic mechanical analysis (DMA). The sample is oscillated in tension, compression, or bend, and the complex modulus is determined from the sample's response to the oscillation. Several commercial vendors offer equipment for making such large-scale measurements. Agilent indentation systems equipped with the CSM option offer the ability to oscillate the indenter. In this way, the complex modulus can be determined from a proper analysis of the contact [1-3]. Instrumented indentation offers two important advantages over DMA in measuring complex modulus. First, the measurement can be made on a spatially-resolved scale, thus allowing one to map out the complex modulus as a function of position. Second, because the moving mass in an indentation system is smaller, the resonant frequency of the equipment is higher, thus allowing a larger frequency range for testing. In this note, we employ dynamic instrumented indentation to measure the complex modulus of highly plasticized polyvinyl chloride (PVC). Results from the present work are compared with previously published results for the same material [4-6]. Terminology is often a significant barrier to understanding a new technique. Therefore, a summary of relevant terms is provided in Table 1.

Table 1. Summary of common terms.

Symbol	Dimensions	Term	Relevance
P	F	Semi-static force	Semi-static force exerted by the indenter on the sample and vice-versa.
h	L	Semi-static displacement	Semi-static penetration of the indenter into the test material, relative to the position at which the indenter first contacted the surface.
$F(t)$	F	Force function	Oscillating force, superimposed upon semi-static force.
$z(t)$	L	Response function	Oscillation of the indenter as a consequence of $F(t)$.
F_O	F	Force amplitude	Amplitude of $F(t)$.
z_O	L	Displacement amplitude	Amplitude of indenter oscillation, $z(t)$.
ω	T^{-1}	Angular frequency	Oscillation frequency
t	T	Time	Abscissa for force and response functions (semi-static and oscillating)
ϕ	-	Phase angle	Angle by which the response function $z(t)$ lags the force function $F(t)$.
m	FT^2L^{-1}	Mass	
D	FTL^{-1}	Damping	
K	FL^{-1}	Stiffness	
i			Subscript: of the indenter
c			Subscript: of the contact
e			Subscript: effective
f			Subscript: of the frame

Agilent Technologies

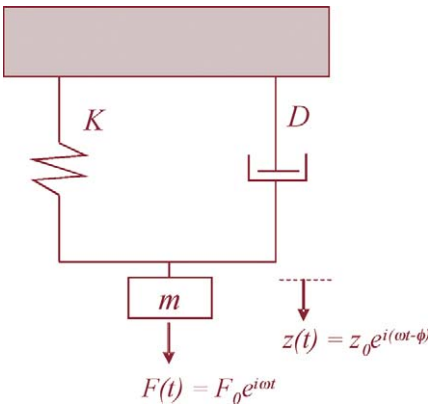

Figure 1. Simple-harmonic oscillator model.

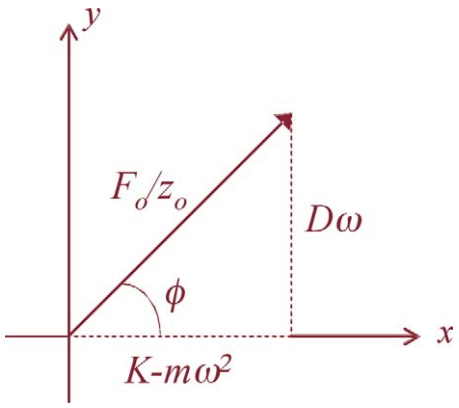

Figure 2. Illustration of solution for system of Figure 1.

Theory

For a thorough literature review and a complete treatment of the theory behind measuring complex modulus by dynamic indentation, the reader should consult reference [4]. In this note, we first review theory for the simple-harmonic oscillator shown in Figure 1. Then we apply this theory to both the equipment and the contact in order to derive expressions for the complex modulus in terms of quantities that are measured during a dynamic indentation experiment [7].

The Simple Harmonic Oscillator

A simple-harmonic oscillator comprises three basic components: a spring of stiffness K, a mass m, and a dashpot with damping coefficient D. If this system is excited by an oscillating force, $F(t) = F_0 e^{i\omega t}$, then we expect a response of the form $z(t) = z_0 e^{i(\omega t-\phi)}$; that is, we expect the oscillation of the mass to be at the same frequency, ω, but lag by a phase angle, ϕ. The second-order differential equation which describes this motion is:

$$m\ddot{z}(t) + D\dot{z}(t) + Kz(t) = F(t). \quad \text{Eq. 1}$$

Taking the first and second derivatives of $z(t)$ yields

$$\dot{z}(t) = z_0 i\omega e^{i(\omega t-\phi)}, \text{ and} \quad \text{Eq. 2}$$

$$\ddot{z}(t) = -z_0 \omega^2 e^{i(\omega t-\phi)}. \quad \text{Eq. 3}$$

Substituting the expressions for z, z', z'', and F into Eq. 1 yields

$$-mz_0\omega^2 e^{i(\omega t-\phi)} + Dz_0 i\omega e^{i(\omega t-\phi)} + Kz_0 e^{i(\omega t-\phi)} = F_0 e^{i\omega t}. \quad \text{Eq. 4}$$

Multiplying every term in Eq. 4 by $e^{i\phi}/(z_0 e^{i\omega t})$ yields

$$-m\omega^2 + iD\omega + K = \frac{F_0}{z_0} e^{i\phi}, \quad \text{Eq. 5}$$

and invoking Euler's rule to substitute for $e^{i\phi}$ yields

$$-m\omega^2 + iD\omega + K = \frac{F_0}{z_0}(\cos\phi + i\sin\phi) \quad \text{Eq. 6}$$

Equating the real parts of Eq. 6 yields

$$K - m\omega^2 = \frac{F_0}{z_0}\cos\phi, \quad \text{Eq. 7}$$

and equating the imaginary parts yields

$$D\omega = \frac{F_0}{z_0}\sin\phi. \quad \text{Eq. 8}$$

So the phase angle, ϕ, by which the response lags the excitation depends on the components through the relationship

$$\tan\phi = \frac{D\omega}{K - m\omega^2}. \quad \text{Eq. 9}$$

This solution is illustrated in Figure 2; by Pythagorean's theorem, we can also express the solution as

$$(K - m\omega^2)^2 + (D\omega)^2 = \left(\frac{F_o}{z_o}\right)^2. \quad \text{Eq. 10}$$

The dynamic compliance, z_0/F_0, is the ratio of the amplitude of the displacement oscillation to the amplitude of the excitation; it has the dimensions of length per unit force. If the system is under-damped, this ratio peaks at resonance; for frequencies greater than the resonant frequency, the value of this ratio decreases monotonically with frequency. Solving Eq. 10 for dynamic compliance yields

$$\frac{z_o}{F_o} = \frac{1}{\sqrt{(K - m\omega^2)^2 + (D\omega)^2}} \quad \text{Eq. 11}$$

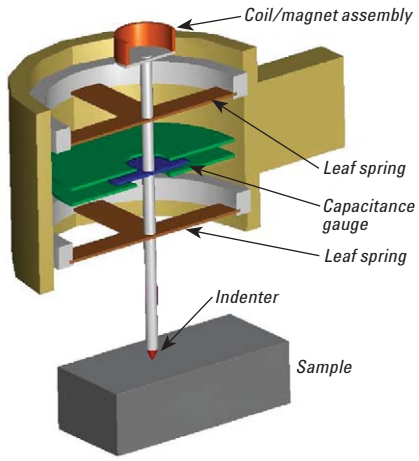

Figure 3. Schematic of the "head" of an Agilent Nanoindenter system.

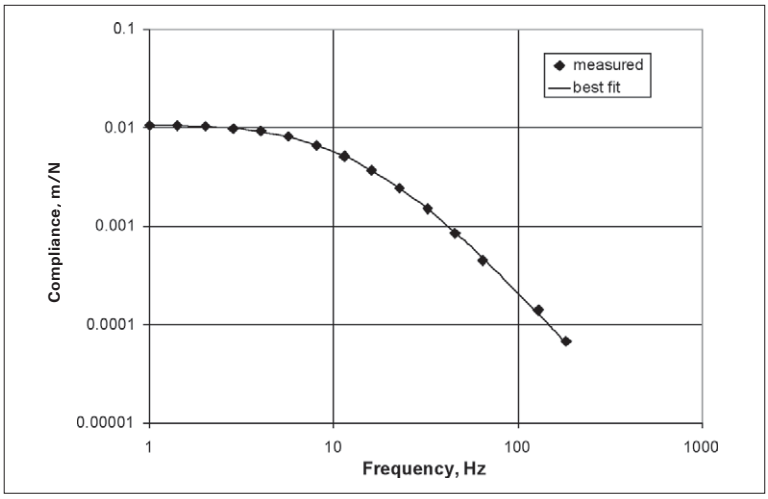

Figure 4. Measured compliance and best fit to Eq. 14 for the Agilent G200 Nanoindenter (XP head). Compliance was measured with the indenter hanging free in the center of its range of travel. Best fit values are K_i = 92.02N/m, m_i = 11.6g, D_i = 2.66N-s/m.

Modeling the Indenter Alone

Let us now apply this model to an indenter that is hanging free. When the indenter is not in contact, the model components are those of the indenter alone: K=K_i, m=m_i, and D=D_i. The springs supporting the indenter shaft are the primary contributors to K_i. If capacitive plates are used for sensing or actuation, they are the primary contributors to D_i. Finally, the mass of indenter shaft is the primary contributor to m_i. Applying Eq. 11 to the case of a free-hanging indenter yields

$$\frac{z_o}{F_o} = \frac{1}{\sqrt{\left(K_i - m_i\omega^2\right)^2 + \left(D_i\omega\right)^2}}, \quad \text{Eq. 12}$$

Logistically, a frequency-specific amplifier (i.e. a "lock-in amplifier") is used to set the amplitude (F_0) and frequency (ω) of the excitation, and also to measure the amplitude of the displacement response (z_0) at the same frequency as well as the phase shift (ϕ) between the two signals.

In order to properly account for the influence of the equipment on the measured response, we must know the components K_i, m_i, and D_i. All Agilent nanoindentation systems are properly represented by the schematic of Figure 3. Semi-static and dynamic forces are imposed electromagnetically. The indenter column is supported by two "leaf" springs that are laterally stiff, but compliant in the direction of indentation. Displacement is measured using a three-plate capacitive arrangement. All three plates are circular disks. The two outside plates are fixed to the head and have holes in the center just large enough to accommodate the indenter shaft. The center plate is fixed to the indenter shaft and is free to move vertically between the two outside plates. The position of the indenter column within the gap is determined by observing the voltage between the center plate and either of the two outside plates. When the indenter is oscillated, the indenter column is the primary contributor to m_i. The supporting springs are the primary contributor to K_i, and the capacitive plates are the primary contributor to D_i.

The values for the model components K_i, m_i, and D_i are determined using a two-step calibration process. The first step is conducted by holding the indenter in the center of its range of travel and oscillating it over a range of frequencies. A plot of compliance vs. angular frequency is generated, and the data are fit to the form of Eq. 12, with K_i, m_i, and D_i as best-fit constants. Such a plot is shown in Figure 4. That the functional form of Eq. 12 fits the data so well is evidence that the simple-harmonic oscillator is a good model for the indenter. The value for m_i determined in this way is a sufficient determination of the effective mass of the indenter. But K_i is generally a weak function of indenter position (because springs are not perfectly linear), and D_i is a strong function of indenter position. Thus, the second step of this process involves determining K_i and D_i as a function of

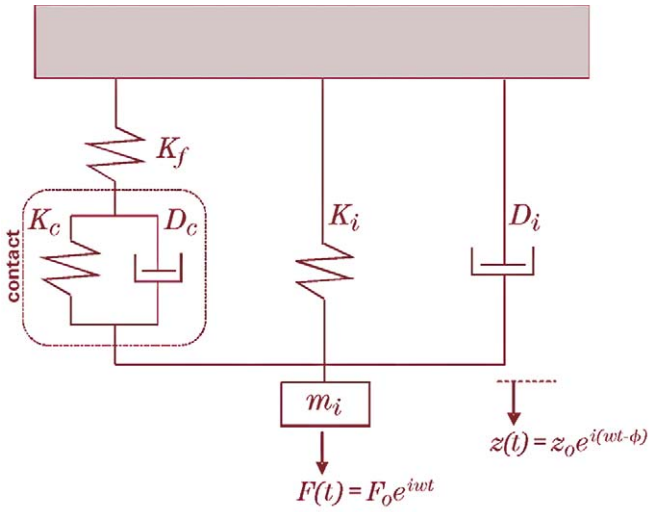

Figure 5. Model accommodating both instrument and contact.

indenter position over its range of travel. This second step is conducted only at the resonance (or natural) frequency.

The fact that the Agilent nanoindentation systems manifest simple-harmonic behavior is not a fortuitous accident, but a design objective. Simple-harmonic behavior requires that the motion occur in only one dimension, with only one mode of oscillation. Atomic-force microscopes (AFMs) that use cantilevered probes do not meet these requirements.

Modeling the Indenter in Contact with a Sample

Now, let us consider the situation when the indenter is in contact with the test material. Components representing the sample have been included in the model shown in Figure 5: K_c and D_c represent the stiffness and damping of the contact, respectively. This material model is adequate if it applied to behavior at a single frequency. When the indenter is in contact, we must account for the elastic stiffness of the frame with the component, K_f.

Components of the equipment and the contact may be combined and represented by effective components such that we can continue to use the simple-harmonic oscillator of Figure 1, with K=K_e and D=D_e; we continue to represent the mass as m_i, because the effective mass is not significantly affected by contact. So the effective components are related to the components representing indenter, frame, and contact by

$$K_e = [1/K_f + 1/K_c]^{-1} + K_i \,, \qquad \text{Eq. 13}$$

and $D_e = D_i + D_c$. Eq. 14

Rearranging these equations to solve for the desired components (the stiffness and damping of the contact) yields

$$K_c = \frac{K_f (K_e - K_i)}{K_f - (K_e - K_i)}$$

(or $K_c = K_e - K_i$ when $K_f >> K_e$) Eq. 15

and $D_c\omega = D_e\omega - D_i\omega$. Eq. 16

Invoking Eqs. 7 and 8 yields

$$K_e - m_i\,\omega^2 = \frac{F_0}{z_0}\cos\phi \,, \text{ and} \qquad \text{Eq. 17}$$

$$D_e\omega = \frac{F_0}{z_0}\sin\phi \,. \qquad \text{Eq. 18}$$

Substituting expressions for K_e (Eq. 17) and K_i (Eq. 12) into Eq. 15 yields the following expression for K_c:

$$K_c = \frac{K_f\left[\frac{F_0}{z_0}\cos\phi - \left(K_i - m_i\,\omega^2\right)\right]}{K_f - \left[\frac{F_0}{z_0}\cos\phi - \left(K_i - m_i\,\omega^2\right)\right]}$$

Eq. 19

Analogously, we calculate the damping of the contact as

$$D_c\omega = \frac{F_0}{z_0}\sin\phi - D_i\omega \,. \qquad \text{Eq. 20}$$

Once the stiffness and damping of the contact have been determined, calculating the components of the complex modulus is straightforward [1-4]:

Figure 6. Highly plasticized PVC (3M EAR C-1002-25) mounted for testing.

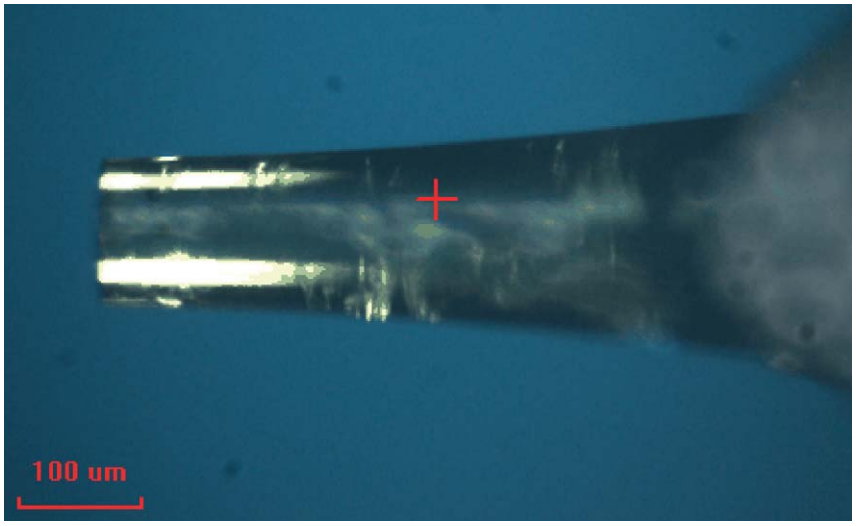

Figure 7. Flat-ended cylindrical punch tip (XP-style holder, 107.1 µm diameter).

$$E' = (1-\nu^2)\frac{K_c}{d}, \text{ and} \qquad \text{Eq. 21}$$

$$E'' = (1-\nu^2)\frac{D_c\omega}{d}, \qquad \text{Eq. 22}$$

where ν and d are the Poisson's ratio of the test material and the diameter of the contact, respectively. The dimensionless loss factor is simply

$$\frac{E''}{E'} = \frac{D_c\omega}{K_c}. \qquad \text{Eq. 23}$$

The expressions for storage and loss modulus depend on the contact diameter, d, so the contact size must be well known in order to accurately determine these properties. But the loss factor does not depend on the geometry of the contact, and so it can be determined even when the contact size is not well known.

Experimental Method

The highly plasticized PVC tested in this work is a product of 3M (EAR C-1002-25). The material is used to provide damping under and around heavy rotating equipment. The material arrived in a small square sheet, approximately six inches on a side and ¼ inch thick. One side of the sheet was mechanically polished to remove a surface layer. Then a 1-inch square was cut from the sheet and mounted on an aluminum puck as shown in Figure 6.

An Agilent G200 Nanoindenter with CSM option and XP-style actuator was used for all testing. The indenter tip was a flat-ended cylindrical punch made of diamond. The punch, shown in Figure 7, had a diameter of 107.1 microns. The advantage of a flat-ended punch for this testing is that the contact area is constant, and not a function of contact depth. The NanoSuite test method "G-Series XP CSM Flat Punch Complex Modulus" was used for this work. This test method brings the indenter into full contact with the test material, oscillates the indenter over a range of frequencies, then applies the analysis described above. Thus, each test yields complex modulus as a function of frequency for a specific test site. Fourteen tests at fourteen different

sites were performed. User-defined inputs were selected to match the test conditions reported by Herbert et al. for the same material [4-5]. Tests were conducted at room temperature.

Results and Discussion

Results for storage modulus and loss factor are shown in Figures 8 and 9. Error bars on the symbols represent one standard deviation on the average. These figures compare the results of the present work with those obtained by Herbert et al. [4-5] for the same material. Herbert et al. employed both DMA (TA Instruments) and indentation (Agilent NanoIndenter XP). For the indentation testing, they used a flat-ended punch of similar diameter (~100 microns). They used a custom indentation test method that was not commercially available.

The agreement between the present results and the indentation results reported by Herbert et al. is excellent. Slight differences, especially at 50Hz, may be explained by the slightly higher temperature for the present results, because the properties of this material are a strong function of temperature [5]. When time-temperature superposition is employed, properties at lower frequencies correspond with properties at higher temperatures.

Given the profound differences in test method and sample geometry, the agreement with DMA is also outstanding. The "wobble" in the DMA results at higher frequencies is likely due to an inadequate accounting for instrument influence, although Herbert et al. report that the instrument was calibrated according to the manufacturer's instructions. The resonant frequency of the instrument

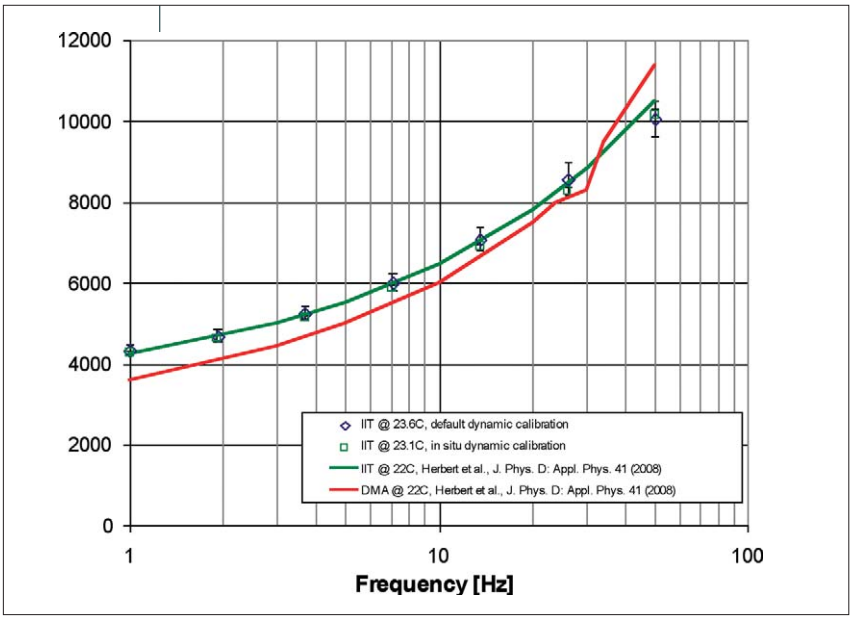

Figure 8. Storage modulus as a function of frequency as determined by default and *in situ* calibration. Results from this work are compared with previously published results obtained by indentation and DMA [4].

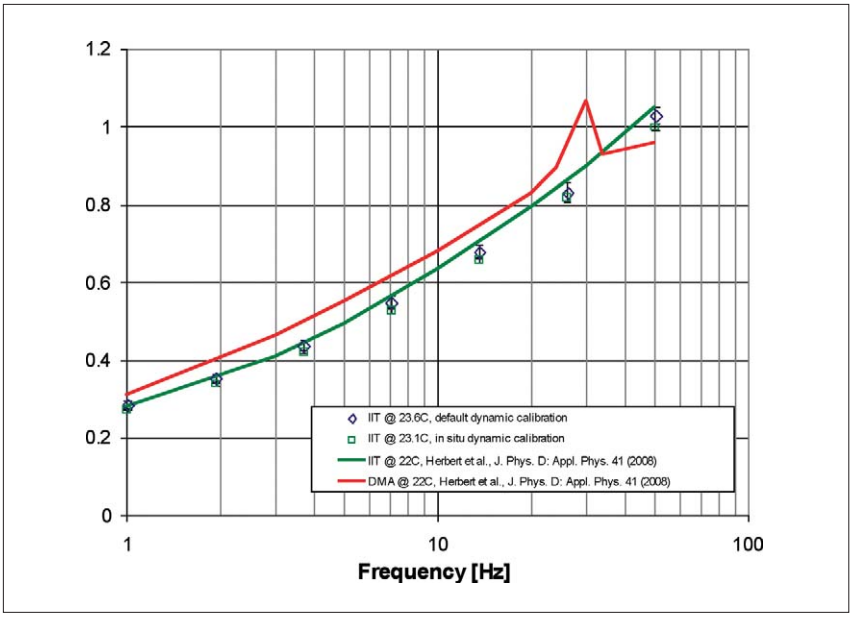

Figure 9. Loss factor as a function of frequency as determined by default and *in situ* calibration. Results from this work are compared with previously published results obtained by indentation and DMA [4].

(whether DMA or indentation) depends inversely on the moving mass. That is, a larger moving mass means a lower resonant frequency. At testing frequencies greater than the resonant frequency, the instrument response becomes progressively more influential–the dynamic stiffness of the instrument increases sharply. Thus, accurately predicting this response becomes progressively more important. Therefore, a testing instrument with a smaller moving mass offers definite experimental advantages.

Conclusions

The Agilent G200 NanoIndenter was successfully used to measure the complex modulus of highly plasticized polyvinyl chloride. Results agreed well with those obtained by others using dynamic mechanical analysis (DMA) and dynamic indentation. Dynamic indentation offers distinct advantages over DMA. First, complex modulus can be measured locally for small volumes of material. Second, instrument calibration is less critical, because a smaller moving mass means that the instrument has a smaller influence on the measurements.

References

1. I.N. Sneddon, "The Relation Between Load and Penetration in the Axisymmetric Boussinesq Problem for a Punch of Arbitrary Profile," *Int. J. Eng. Sci.,* Vol. 3, pp. 47–56, 1965.
2. W.C. Oliver and G.M. Pharr, "An Improved Technique for Determining Hardness and Elastic Modulus Using Load and Displacement Sensing Indentation Experiments," *J. Mater. Res.,* Vol. 7 (No. 6), pp. 1564–1583, 1992.
3. J-L. Loubet, B.N. Lucas, W.C. Oliver, "Some measurements of viscoelastic properties with the help of nanoindentation," *NIST Special Publication,* Vol. 896, pp. 31–34, 1995.
4. E.G. Herbert, W.C. Oliver, and G.M. Pharr, "Nanoindentation and the dynamic characterization of viscoelastic solids," *J. Phys. D: Appl. Phys.,* Vol. 41, pp. 1–9, 2008. (Full text: http://www.iop.org/EJ/abstract/0022-3727/41/7/074021/)
5. E.G. Herbert, W.C. Oliver, A. Lumsdaine, G.M. Pharr, "Measuring the constitutive behavior of viscoelastic solids in the time and frequency domain using flat punch indentation," *J. Mater. Res.,* Vol. 24 (No. 3), 2009. (Abstract: http://www.mrs.org/s_mrs/sec_subscribe.asp?CID=14100&DID=232328&action=detail)
6. http://en.wikipedia.org/wiki/Polyvinyl_chloride
7. J.L. Hay, P. Agee, E.G. Herbert, "Continuous stiffness measurement during instrumented indentation testing," *Experimental Techniques,* January 2010. (First page: http://dx.doi.org/10.1111/j.1747-1567.2010.00618.x)

Nano Mechanical Systems from Agilent Technologies

Agilent Technologies, the premier measurement company, offers high-precision, modular nano-measurement solutions for research, industry, and education. Exceptional worldwide support is provided by experienced application scientists and technical service personnel. Agilent's leading-edge R&D laboratories ensure the continued, timely introduction and optimization of innovative, easy-to-use nanomechanical system technologies.

www.agilent.com/find/nanoindenter

Americas

Canada	(877) 894 4414
Latin America	305 269 7500
United States	(800) 829 4444

Asia Pacific

Australia	1 800 629 485
China	800 810 0189
Hong Kong	800 938 693
India	1 800 112 929
Japan	0120 (421) 345
Korea	080 769 0800
Malaysia	1 800 888 848
Singapore	1 800 375 8100
Taiwan	0800 047 866
Thailand	1 800 226 008

Europe & Middle East

Austria	43 (0) 1 360 277 1571
Belgium	32 (0) 2 404 93 40
Denmark	45 70 13 15 15
Finland	358 (0) 10 855 2100
France	0825 010 700*
	*0.125 €/minute
Germany	49 (0) 7031 464 6333
Ireland	1890 924 204
Israel	972-3-9288-504/544
Italy	39 02 92 60 8484
Netherlands	31 (0) 20 547 2111
Spain	34 (91) 631 3300
Sweden	0200-88 22 55
Switzerland	0800 80 53 53
United Kingdom	44 (0) 118 9276201

Other European Countries:
www.agilent.com/find/contactus

Printed in USA, July 29, 2010
5990-6330EN

Agilent Technologies